ISSN: 2281-1346

Department of Economics and Management

DEM Working Paper Series

Bifurcation structure in a bimodal piecewise linear business cycle model

Viktor Avrutin
(Università di Urbino)

Iryna Sushko
(National Academy of Sciences of Ukraine)

Fabio Tramontana
(Università di Pavia)

 # 76 (04-14)

Via San Felice, 5
I-27100 Pavia
http://epmq.unipv.eu/site/home.html

April 2014

Bifurcation structure in a bimodal piecewise linear business cycle model

Viktor Avrutin,[a] *Iryna Sushko,*[b] *Fabio Tramontana*[c*]

[a]DESP, University of Urbino, Italy and IST, University of Stuttgart, Germany
[b]Institute of Mathematics, National Academy of Sciences of Ukraine
[c]Department of Economics and Management, University of Pavia, Italy

Abstract

We study the bifurcation structure of the parameter space of a 1D continuous piecewise linear bimodal map which describes dynamics of a business cycle model introduced by Day-Shafer. In particular, we obtain the analytical expression of the boundaries of several periodicity regions associated with attracting cycles of the map (principal cycles and related fin structure) crossing which the map has robust chaotic behavior.

1 Introduction

Applied models defined by *piecewise smooth* functions appear quite often when one studies a real process characterized by some 'nonsmooth' phenomena such as sharp switchings between several states, impacts, friction, sliding, and the like. In economic modeling piecewise smooth systems arise, for example, taking into account that the most used economic variables have non-negativity constraints, or when a process is studied in which the economic agents change their behavior when a relevant indicator reaches certain thresholds, etc. The main reason why economists still prefer to build their theoretical models avoiding piecewise smooth functions is related to the lack of knowledge and experience in the investigation of such a kind of models. In fact, a general theory for piecewise smooth dynamical systems, differently from the one for smooth systems, is not yet well established. The studies and results on these systems are growing and rapidly developing nowadays (see, e.g., the books [29], [4] and references therein). During the last decade important results have been obtained in this field, and one of the aims of the present paper is to show that such results can be successfully applied to investigate a relevant economic model, proposed by Day and Shafer in [9].

*Corresponding Author: University of Pavia, Department of Economics and Management, Via S.Felice 5, 27100 Pavia (PV), Italy. email: fabio.tramontana@unipv.it

We recall that among nonsmooth dynamical systems, those described by piecewise linear maps are the simplest to study due to the linearity of their components, but nevertheless they are quite rich in the outcome of the possible dynamics. In particular, a one-dimensional (1D for short) continuous piecewise linear map with one border point, known as *skew tent map,* depending on the parameters values can have attracting cycles of any period as a well as cyclic chaotic intervals of any period, also called $n-$bands chaotic attractors, which have the relevant property of being robust (as introduced in [3]) with respect to parameter perturbations. The bifurcation structure of the skew tent map has been completely described (see, e.g., [15], [28], [19], [25]). Moreover, the skew tent map can be used as a normal form for a so-called *border collision bifurcation* (BCB for short) which is characteristic in piecewise smooth maps ([22], [2]). Recall that a BCB occurs when an invariant set, such as, for example, a fixed point or cycle, collides with a border separating regions of different definition of the map. This bifurcation may lead, for example, from an attracting cycle directly to chaos. The dynamic behaviors of the skew tent map are used to classify the possible dynamics which may occur after a generic BCB in a 1D continuous piecewise smooth map (see, e.g., [26], [12], [27], where the skew tent map is applied to classify BCBs in economic models).

The map considered in the present paper, which represents an economic model, is described by a one-dimensional (1D for short) *bimodal piecewise linear map* with increasing outermost branches. Clearly, a map with two border point possesses more complicated dynamics, and all the possible outcomes are not yet fully investigated, some results can be found in [20] and [23]. In particular, the bifurcation structure of its parameter space includes both regions which belong to the known *period adding structure* (called also *Arnold tongues* or *mode-locking tongues*), which is characteristic for piecewise increasing discontinuous maps and also for certain circle maps (see, e.g. [17], [16], [5], [1], [10]). The period adding structure is formed by periodicity regions related to cycles organized according to the Farey summation rule applied to the rotation numbers of the related cycles. Besides this, in bimodal piecewise linear maps the so-called *fin structure* is also observed (see [23]). We shall describe these regions in the parameter space of the considered map, recalling how these two structures are organized, and giving formulas of the boundaries of related regions.

The plan of the work is as follows. In Section 2 we recall the Day-Shafer model. Its dynamics are bounded in an absorbing interval, and depending on the parameters values the system may have attracting cycles of any period as well as n-band chaotic attractors. In Section 3 we shall consider the parameter space of interest, showing how the periodicity regions representing the regions in the parameter space associated with stable attracting cycles may be organized. Moreover, the boundaries of such regions (BCB curves) are obtained analytically (and reported in Appendices). Crossing these boundaries the system may either enter a different periodicity region (via the fin structure mentioned above) or it may become chaotic (and in a regime of robust chaos). Some conclusions are given in Section 4.

2 The Day-Shafer model

The Day-Shafer model we are interested in dates back to 1987. Richard Day has been a pioneer in the application of nonlinear models in economics and finance (see e.g. [6], [7], [8], [14]). In particular, in [9] Day and Shafer argued that the trapping set of their nonlinear business cycle model in one of the most interesting cases is well approximated by a piecewise smooth map with two *turning points* with dynamics bounded in an absorbing interval. Moreover, they explicitly consider a piecewise linear bimodal map as a further approximation. In the particular case in which the dynamics reduces to those on a unimodal piecewise linear map (i.e. a skew tent map), they succeeded in writing the BCB curves associated with the principal (or maximal) cycles. While in the generic case of a piecewise linear bimodal map, only a few numerical results were given. As we shall show in the next sections, the results of the generic case with two turning points can be much improved and many BCB curves can be detected analytically.

Let us briefly recall that in [9] Day and Shafer build a generic map defining a business cycle model of an economy with monetary and real sectors. In the monetary market, demand and supply for money are implicitly given by the interest rate r as a function of the income Y and a money supply parameter M. In the real market the interest rate determines the level of investments $I = H(r(Y), Y) = I(Y)$, that is a component of the income together with consumption $C = C(Y)$. By using the assumption that the level of income at a certain time period depends upon the one-time lagged amounts of consumption and investment, it is obtained a discrete time equation of the following form:

$$Y_{t+1} = F(Y_t) = \lambda I(Y_t) + C(Y_t) + A, \tag{1}$$

where the parameter $\lambda \geq 0$ measures how strongly investment translates into new income, and the parameter $A > 0$ includes all the autonomous components (of investment, consumption and public expenditure). The function $C(Y)$ is typically monotonically increasing with $C(0) = 0$, the investment function $I(Y)$ usually is increasing for low level of income while it is decreasing when income is high[1]. Putting together these assumptions a function $F(Y)$ is obtained that is nonlinear and has a bimodal shape. By using explicit functions, Day and Shafer found that for some parameters' configurations the income dynamics are bounded in a trapping set like the one shown in Fig.1. The piecewise linear map shown in Fig.1 represents the function $F(Y)$, it is continuous but not differentiable at the points $Y = Y^*$ and $Y = Y^{**}$. The dynamics are bounded in the interval $[F(Y^{**}), F(Y^*)] = \left[Y^m, Y^M\right]$. For convenience, we can normalize the interval $\left[Y^m, Y^M\right]$ to $[0, 1]$ and denoting by x the state variable income Y

[1] This is due to the fact that with high income the money market becomes too crowded, inducing the increase of the interest rate that causes a contraction in the investments.

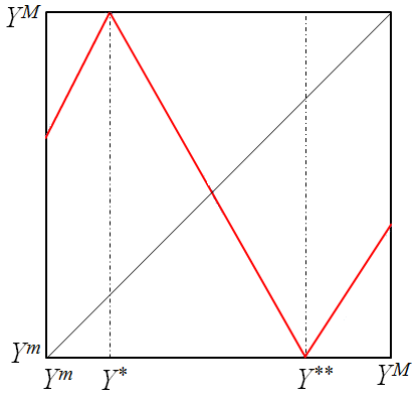

Figure 1: The function $F(Y)$ in the trapping interval $\left[Y^m, Y^M\right]$.

we obtain the map $f : I \to I$, $I = [0, 1]$ defined as follows:

$$f : x \mapsto f(x) = \begin{cases} f_L(x) = a_L x + 1 - a_L d_L & \text{if} \quad 0 \le x < d_L, \\ f_M(x) = -\dfrac{x}{d_R - d_L} + 1 + \dfrac{d_L}{d_R - d_L} & \text{if} \quad d_L \le x < d_R, \\ f_R(x) = a_R x - a_R d_R & \text{if} \quad d_R \le x \le 1. \end{cases} \tag{2}$$

where $f_L(d_L) = f_M(d_L) = 1$, $f_R(d_R) = f_M(d_R) = 0$ and the parameters satisfy

$$a_L > 0,\ a_R > 0,\ 0 < d_L < d_R < 1,\ f(0) > 0,\ f(1) < 1 \tag{3}$$

so that $f(I) = I$. More correctly, this is a version of the map in which we can investigate the dynamic behavior changing independently the slopes of the external branches and border points. In [9] the authors give the relations between the parameters here considered and those related to the economic model. Moreover, the parameters used above (slopes and border points) may all or in part depend on some economic parameters, so that as an economic parameter is varied, it is also possible that it influences several of the above parameters, leading to particular paths in the parameter space.

Clearly, this map (2) has a unique fixed point in the middle branch given by

$$x_M^* = \frac{1 + d_R}{1 + d_R - d_L} \tag{4}$$

which is always unstable given that the slope of the middle branch $(-\dfrac{1}{d_R - d_L})$ is always smaller than -1. The interval I is trapping so in I we do not have any divergent trajectory, and the attracting set may be periodic (an $n-$cycle with $n > 1$) or chaotic (a chaotic interval or an $n-$band chaotic attractor with $n > 1$). Some dynamic behaviors and bifurcation structures of map (2) will be described in the next Section.

3 Bifurcation structure of the parameter space

3.1 Preliminaries

The Day-Shafer model presented in the previous section is described by a family of 1D continuous piecewise linear maps $f : I \to I$, $I = [0, 1]$, as given in (2), where the parameter region of interest, which allows to obtain the required shape of the map, is the region P defined as follows (as $f(0) > 0$ leads to $a_L d_R < 1$ while $f(1) < 1$ leads to $a_R(1 - d_R) < 1$)):

$$P = \{p : a_L > 0,\ a_R > 0,\ 0 < d_L < d_R < 1,\ a_L d_R < 1,\ a_R(1 - d_R) < 1\}, \quad (5)$$

where $p = (a_L, a_R, d_L, d_R)$ denotes a point in the parameter space. For $p \in P$ the left and the right branches of map f are both increasing, while the middle one is decreasing, so that f is a *bimodal* map. An example is shown in Fig.2. As already mentioned in the Introduction, the dynamics of 1D bimodal maps have been considered by many researchers (see, e.g., [18], [21], [20], [24], etc.). Our aim is to study the bifurcation structure of the region P, that is, to describe the possible attractors of map f and the parameter regions corresponding to their existence.

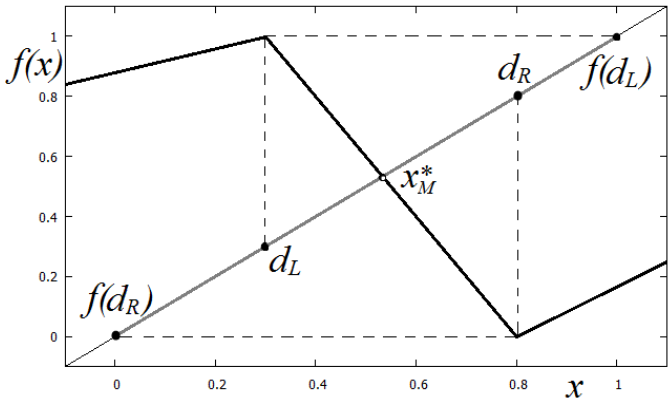

Figure 2: The map f given in (2) for $a_L = 0.4$, $a_R = 0.8$, $d_L = 0.3$, $d_R = 0.8$.

Let us denote as $I_L = [0, d_L)$, $I_M = [d_L, d_R)$ and $I_R = [d_R, 1]$ the definition intervals (or, in other words, *partitions*) of the functions f_L, f_M and f_R, respectively. They are separated by the *border points* d_L and d_R. As already remarked, for $p \in P$ the fixed point is $x^*_M \in I_M$ as given in (4) always exists and is *repelling*, while the fixed points

$$x^*_L = \frac{a_L d_L - 1}{a_L - 1},\ x^*_R = \frac{a_R d_R}{a_R - 1}, \quad (6)$$

associated with the branches f_L and f_R, exist (repelling) for $a_L > 1$ and $a_R > 1$. However, for the considered parameter values these fixed points do not belong

to the interval I given that $x_L^* < 0$ and $x_R^* > 1$. For our map f the absorbing interval is always associated with all three branches. In fact, given that $f(d_L) = 1 > d_R$ and $f(d_R) = 0 < d_L$ it follows that I is an *absorbing interval* and invariant, $f(I) = I$ (see Fig.2), so that any orbit with an initial value $x_0 \in I$ is *bounded,* being trapped in I. We denote by φ_L and φ_R the boundaries related to the contact of the interval I with the fixed points x_L^* and x_R^*, given by $x_L^* = 1$ and $x_R^* = 1$, respectively (although not occurring for parameters in P):

$$\varphi_L : \ a_L d_R = 1, \tag{7}$$

$$\varphi_R : \ a_R(1 - d_R) = 1. \tag{8}$$

Suppose that $\{x_i\}_{i=1}^n$ are the points of an n-cycle of map f. The symbolic representation of such a cycle is $\sigma = s_1 s_2 ... s_n$, obtained associating to each point x_i the symbol $s_i \in \{L, M, R\}$ depending on the partition I_L, I_M or I_R which the point x_i belongs to. In the following, to denote an n-cycle we use its symbolic representation. The region in the parameter space related to the existence and stability of a cycle with symbolic sequence σ is denoted P_σ, and called *periodicity region.* Clearly, the boundaries of a periodicity region can be related either to the stability loss of the cycle due to its eigenvalue crossing ± 1 (recall that for a piecewise linear map such bifurcations are *degenerate*, see [25]), or to the appearance/disappearance of the cycle due to a *border collision bifurcation* (see [22]). We recall that if some point of a cycle collides with a border point and neither the period nor the stability of the cycle changes after the collision, we say that this cycle undergoes a *persistence border collision*, while a *border collision bifurcation* (BCB) occurs when a qualitative change in the dynamics is observed after the collision.

As noticed in [23], the overall bifurcation structure of the parameter space for a generic 1D bimodal piecewise linear map is characterized by several substructures among which we recall the skew tent map structure, the period adding structure and a particular one called fin structure (due to the shape of the periodicity regions, as it will be clear below). The simplest one is the *skew tent map structure* associated with absorbing intervals involving only two adjacent partitions, so that on these absorbing intervals the map is reduced to a skew tent map. However, as already mentioned, by definition for our map f such a possibility is excluded. That is, the parameter space of f does not include the skew tent map structure. The *period adding structure* is associated with periodicity regions related to attracting cycles whose points belong to the outermost partitions only. Such periodicity regions are ordered according to the Farey summation rule applied to the rotation numbers of the related cycles. This bifurcation structure is observed for our map f and we describe it in detail in Sec.3.3. The *fin structure* which also reveals itself in the parameter space of map f (see Sec.3.4) is closely related to the period adding structure being formed by the periodicity regions contiguous to the regions of the period adding structure and related to attracting cycles with just one point belonging to the middle partition and all the other points belonging to the outermost partitions.

3.2 Two-dimensional bifurcation diagrams

We first present a few 2D bifurcation diagrams in various parameter planes to illustrate the overall bifurcation structure of the parameter space of map f. In particular, Fig.3 shows such a diagram and its enlargement in the (a_L, a_R)-parameter plane for $d_L = 0.4$, $d_R = 0.8$, $0 < a_L < 1/d_L = 2.5$, $0 < a_R < 1/(1-d_R) = 5$. Here different colors are related to attracting cycles of different periods $n \leq 30$, where the correspondence of a color and the period is indicated in the color bar, white region corresponds either to chaotic attractors or to cycles of higher periodicity. The gray region corresponds to $a_L > 1$, $a_R > 1$, so that all the slopes of f are larger than 1 in modulus, thus, attracting cycles can not exist, and it is associated with chaotic attractors only (cyclic chaotic intervals).

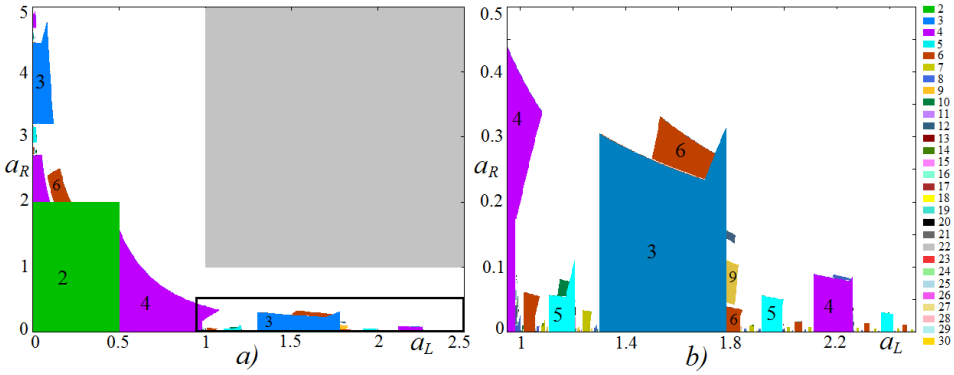

Figure 3: 2D bifurcation diagram of the map f in the (a_L, a_R)-parameter plane in *(a)*, at $d_L = 0.4$, $d_R = 0.8$, and an enlargement of the indicated window in *(b)*. The color bar indicates the correspondence of a color and the period of the related cycle.

The choice of the parameters a_L and a_R to be varied for fixed values of d_L and d_R, as in Fig.3, is not optimal to illustrate the bifurcation structures typical for piecewise linear bimodal maps. To this purpose it is better to fix values for a_L and a_R, and vary d_L and d_R, as it is shown in Figs.4 and 5. In these figures, the characteristic shapes of the periodicity regions belonging to the period adding structure are visible. Such regions have one side on the straight line $d_L = d_R$, and also are observable regions which are contiguous (or attached) to the regions of the period adding structure, and are those constituting the 'fin structure'. A third example in the (d_L, d_R)-parameter plane is shown in Fig.5 at $a_L = 0.7$ and $a_R = 0.8$ fixed. We shall see how to get the analytic equations of the BCB curves bounding the periodicity regions evidenced in the figures.

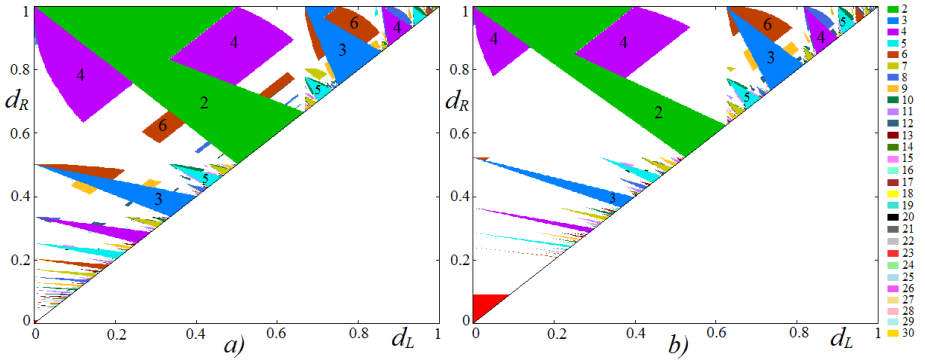

Figure 4: 2D bifurcation diagram of f in the (d_L, d_R)-parameter plane for $a_L = 0.5$, $a_R = 1.01$ in *a)*, and $a_L = 0.6$, $a_R = 1.1$ in *b)*. Here the red region defined by $d_L < d_R < 1 - 1/a_R$, is related to divergent orbits, and not involved in the economic model.

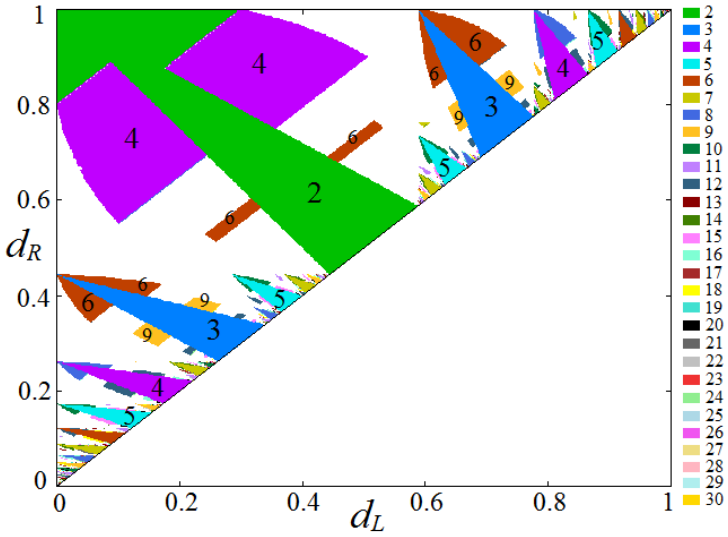

Figure 5: 2D bifurcation diagram of f in the (d_L, d_R)-parameter plane for $a_L = 0.7$, $a_R = 0.8$.

3.3 Period adding structure

Let us briefly recall the main elements of the period adding structure. As already mentioned, the periodicity regions constituting this structure are related to attracting n-cycles, $n \geq 2$, whose points only belong to the partitions I_L and I_R, that is, their symbolic sequences does not include the symbol M.

Following [17] all the cycles associated with the period adding structure are grouped into families according to *complexity levels*. The *complexity level one* includes two families, denoted $\Sigma_{1,1}$ and $\Sigma_{2,1}$, to which the so-called *basic* cycles belong:

$$\Sigma_{1,1} = \{LR^{n_1}\}_{n_1=1}^{\infty}\,, \quad \Sigma_{2,1} = \{RL^{n_1}\}_{n_1=1}^{\infty}\,. \tag{9}$$

Note that the 'central' cycle $LR \equiv RL$ belongs to both families. To get the symbolic sequences of the cycles of families of *complexity level two* we apply to the families $\Sigma_{1,1}$ and $\Sigma_{2,1}$ the following *symbolic replacements:*

$$\kappa_m^L := \left\{ \begin{array}{l} L \to LR^m \\ R \to RLR^m \end{array} \right. , \quad \kappa_m^R := \left\{ \begin{array}{l} L \to LRL^m \\ R \to RL^m \end{array} \right. . \tag{10}$$

This method is based on the *map replacement technique* (see [1], [10]). Namely, at first we substitute in $\Sigma_{1,1}$ each symbol L by LR^m and each symbol R by RLR^m (replacement κ_m^L), and then we substitute in $\Sigma_{1,1}$ each symbol L by LRL^m and each symbol R by RL^m (replacement κ_m^R). Then the index m is set $m = n_2$ in order to write the two families of complexity level two, respectively, as follows:

$$\Sigma_{1,2} = \{LR^{n_2}\,(RLR^{n_2})^{n_1}\}_{n_1,n_2=1}^{\infty}\,, \quad \Sigma_{2,2} = \{LRL^{n_2}\,(RL^{n_2})^{n_1}\}_{n_1,n_2=1}^{\infty}\,. \tag{11}$$

We notice that the replacement technique is here used to detect the symbolic representation of the existing cycles. However, the same technique is used also to get the equations of the BCB curves of cycles of complexity level higher than one, starting from the equations of those of complexity level one.

Similarly, applying the replacements κ_m^L and κ_m^R to $\Sigma_{2,1}$ we get the symbolic sequences of two more families:

$$\Sigma_{3,2} = \{RLR^{n_2}\,(LR^{n_2})^{n_1}\}_{n_1,n_2=1}^{\infty}\,, \quad \Sigma_{4,2} = \{RL^{n_2}\,(LRL^{n_2})^{n_1}\}_{n_1,n_2=1}^{\infty}\,. \tag{12}$$

Note that the central cycle $LRRLR \equiv RLRLR$ belongs to both families $\Sigma_{1,2}$ and $\Sigma_{3,2}$, with $n_1 = n_2 = 1$, while the central cycle $LRLRL \equiv RLLRL$ belongs to both families $\Sigma_{2,2}$ and $\Sigma_{4,2}$, with $n_1 = n_2 = 1$. All the other cycles in these families are distinct. In short this procedure can be written as $\Sigma_{1,2} = \kappa_{n_2}^L(\Sigma_{1,1})$, $\Sigma_{2,2} = \kappa_{n_2}^R(\Sigma_{1,1})$, $\Sigma_{3,2} = \kappa_{n_2}^L(\Sigma_{2,1})$ and $\Sigma_{4,2} = \kappa_{n_2}^R(\Sigma_{2,1})$. So, we get 4 families of complexity level two[2]. Further, applying the replacements (10) with $m = n_3$ to the families of complexity level two we obtain 2^3 families $\Sigma_{j,3}$, $j = 1, \ldots, 2^3$,

[2] One more way to construct the families of the complexity level two consists in consequtive application of the concatenation rule to the 'neighbour' symbolic sequences of the first complexity level. Symbolic sequences obtained in such a way are shift invariant to those obtained by symbolic replacements (10) (see [1], [10]).

of *complexity level three,* and so on. In this way all the symbolic sequences of cycles associated with the period adding structure are obtained.

Now let us turn to the boundaries of the periodicity regions (i.e. the BCB curves) related to the cycles of map f associated with the period adding structure. They can be confined by the boundaries related to their existence, crossing which a cycle disappears, which are related to the BCBs occurring when a point of the cycle close to a border point, $x = d_L$ or $x = d_R$, collides with it in a saddle-node border collision bifurcation (merging with a companion unstable cycle). For the boundaries of a periodicity region associated with the stability of the cycle, first note that an n-cycle whose symbolic sequence σ does not include the symbol M, has multiplier $\lambda_\sigma = a_L^k a_R^{n-k} > 0$, where k and $n-k$ are the numbers of symbols L and R, respectively, in σ. Thus, a degenerate flip bifurcation (DFB for short), related to $\lambda_\sigma = -1$, can not occur for such a cycle, so that the periodicity regions of the period adding structure cannot have DFB boundaries. A degenerate $+1$ bifurcation (DB1 for short) associated with $\lambda_\sigma = 1$ occurs if $a_L^k a_R^{n-k} = 1$. Obviously, this condition defines a boundary of the periodicity region only if the related cycle exists.

To illustrate how the periodicity regions of the period adding structure are ordered let us consider first the limit case $d_L = d_R \equiv d$ at which the considered map becomes discontinuous, say $\widetilde{f}$:

$$x \mapsto \widetilde{f}(x) = \begin{cases} \widetilde{f}_L(x) = a_L x + 1 - a_L d & \text{if} \quad 0 \le x < d, \\ \widetilde{f}_R(x) = a_R x - a_R d & \text{if} \quad d < x \le 1, \end{cases} \tag{13}$$

In Figs.4 and 5, when the parameters belong to the straight line $d_L = d_R$ then the smooth map f reduces to the discontinuous one, $\widetilde{f}$.

The dynamics of 1D discontinuous piecewise monotone maps have been studied by many researchers (see, e.g., [16], [13], [5], [11]). In particular, the piecewise linear case has been recently reconsidered (after [17]) in [1] and [10]. In the cited references, it is described the period adding structure which is characteristic for piecewise increasing maps, when invertible on the absorbing interval. It is easy to check that map $\widetilde{f}$ is invertible on the absorbing interval I if $f_L(f(d)) > f_R(f(d))$, that is, if $f_L(0) > f_R(1)$, in which case $\widetilde{f}$ is called *gap map*. It is noninvertible if $f_L(0) < f_R(1)$ being also called *overlapping map*, while for $f_L(0) = f_R(1)$ map $\widetilde{f}$ is called *circle map*. The boundary defined by $f_L(0) = f_R(1)$, that holds for

$$\kappa = \{(a_L, a_R, d) : a_L > 0,\ a_R > 0,\ 0 < d < 1,\ 1 - d a_L = a_R(1-d)\}, \tag{14}$$

is related to the changes of invertibility of $\widetilde{f}$. In Fig.6 we show the 2D bifurcation diagram of $\widetilde{f}$ in the (d, a_R)-parameter plane for $a_L = 0.5$, and the curve κ is there plotted. Note that the dynamics along the straight line defined by $a_R = 1.1$ is related to the dynamics along the straight line $d_L = d_R$ in Fig.4*a*. Below the curve κ one can observe the period adding structure. Above the curve φ_R given in (8) a generic trajectory of $\widetilde{f}$ diverges, while in between φ_R and κ the existing attractors of map are chaotic intervals.

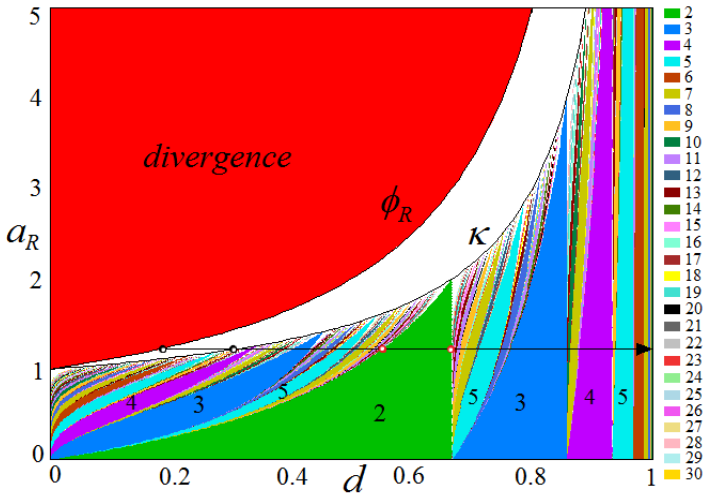

Figure 6: 2D bifurcation diagram of map $\widetilde{f}$ in the (d, a_R)-parameter plane for $a_L = 0.5$.

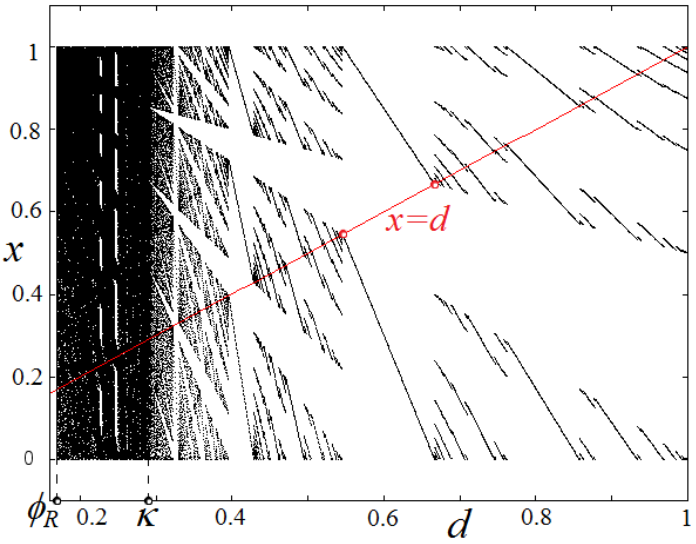

Figure 7: 1D bifurcation diagram of map $\widetilde{f}$ for $a_L = 0.5$, $a_R = 1.2$, $d \in (\varphi_R, 1)$, where $\varphi_R \approx 0.167$. The related parameter path is indicated in Fig.6 by the horizontal line with an arrow.

The period adding structure in map $\widetilde{f}$ is illustrated by the 1D bifurcation diagram in Fig.7 corresponding to the cross-section along the horizontal line with an arrow indicated in Fig.6. Note that for $\varphi_R < d < \kappa$, where $\varphi_R \approx 0.167$, $\kappa \approx 0.286$, the attractor is chaotic. It can be also clearly seen that the boundaries of the periodicity regions, for example of the 2-cycle, are related to the collision of the points of the cycle with the border point $x = d$.

In Appendix A we give the analytic equations of the boundaries of the periodicity regions of the period adding structure for map f, which holds also for map $\widetilde{f}$ substituting $d_L = d_R = d$. The periodicity regions of complexity level one and two of map f, corresponding to the bifurcation diagram presented in Fig.5 are shown in Fig.8 by light gray and dark gray regions, respectively. In that figure, the boundaries of the gray regions are plotted using the formulas given in Appendix A. For example, after simplifications we get that periodicity region P_{RL} related to the attracting 2-cycle RL of map f is defined as follows:

$$P_{RL} = \left\{ p \in P : 1 - \frac{d_L}{a_R} < d_R < 1 - a_L d_L \right\}, \tag{15}$$

and the equations $d_R = 1 - \dfrac{d_L}{a_R}$, $d_R = 1 - a_L d_L$ define the two BCB curves giving the boundaries of P_{RL}. For fixed $d_L = 0.4$, $d_R = 0.8$, as in Fig.3, the boundaries of P_{RL} are just segments of the vertical and horizontal straight lines defined by $a_L = \dfrac{1 - d_R}{d_L} = 0.5$ and $a_R = \dfrac{d_L}{1 - d_R} = 2$, respectively.

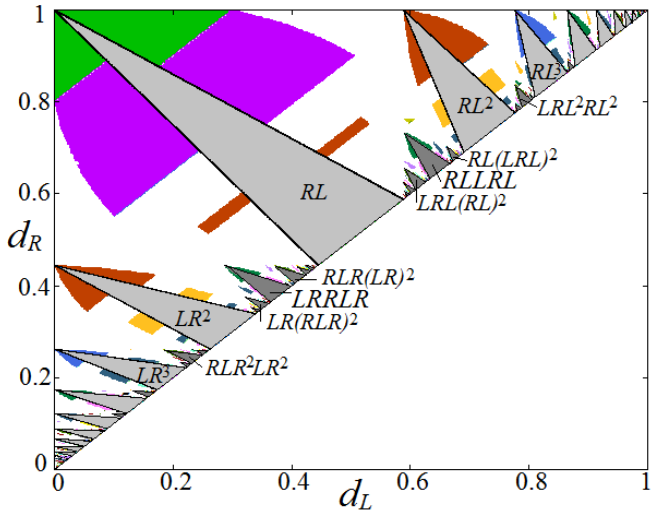

Figure 8: Periodicity regions of the cycles LR^n and RL^n, $n = 1, ..., 11$, of complexity level one are shown in light gray. A few periodicity regions of complexity level two are shown in dark gray. Here $a_L = 0.7$, $a_R = 0.8$ as in Fig.5.

3.4 Fin structure

As already mentioned, the fin structure in the parameter space of a 1D bimodal piecewise linear map consists of periodicity regions which are attached to the regions of the period adding structure described in the previous section. For example, one can clearly see in Fig.5 two $2 \cdot 2$-periodicity regions and two $2 \cdot 3$-periodicity regions attached on both sides to the period-2 region P_{RL}, as well as $3 \cdot 2$-, $3 \cdot 3$- and $3 \cdot 4$-periodicity regions attached on both sides to the period-3 regions P_{RL^2} and P_{LR^2}, and so on. These regions belong to the fin structure which is formed by the periodicity regions called $n \cdot k$-fins, $k \geq 1$, related to attracting cycles having only one point in the interval I_M and all the other points are in I_L and I_R. The n-periodicity region of the period adding structure to which a fin is attached is called *trunk* region, and its fins have the same complexity level as the complexity level of the trunk. In fact, in Fig.5 it can be seen also two $2 \cdot 1$-fins of complexity level one of the trunk regions P_{RL}.

A fin cycle can appear if the parameter point crosses one of two BCB boundaries of a trunk, due to which one periodic point enters the partition I_M. As explained in [23], for an $n \cdot k$-cycle whose periodicity region has the common boundary with the region $P_{LR^{n-1}}$, the symbolic sequences of the cycles in the fins are $(LR^{n-1})^{k-1}MR^{n-1}$, $k = 1, 2, ...$, on one side of the region $P_{LR^{n-1}}$, and $(LR^{n-1})^{k-1}LR^{n-2}M$ on the other side. Interchanging L and R in these sequences we get the symbolic sequences of the cycles related to $n \cdot k$-fins whose trunks are $P_{RL^{n-1}}$ regions. The number of existing fins depends on the parameters and, in fact, some trunk regions may have fins on one side only, or have no fins at all, as can be seen, for example, in Fig.4*b*.

As for the boundaries of a fin, it can be shown that each $n \cdot k$-fin region for $k \geq 2$, $n \geq 2$, related to a cycle with symbolic sequence σ, has at most four boundaries, among which one is the common BCB boundary with the related trunk region, one boundary is related to DFB of the cycle (whose eigenvalue is $\lambda_\sigma = a_L^m a_R^{nk-m-1}/(d_L - d_R) < 0$, where m is the number of symbols L in σ) and two other boundaries are related to two more BCBs of the cycle. Each $n \cdot 1$-fin region has only three boundaries, namely, one DFB boundary and two BCB boundaries. The DFB boundary is defined by the condition $\lambda_\sigma = -1$, while the BCB boundaries are obtained using the skew tent map as border collision normal form.

In Appendix B, some basic formulas related to the boundaries of a fin region are given, while below, as an example, we describe the $2 \cdot 1$- and $2 \cdot 2$-fins of the region P_{RL} shown in Fig.9. There are two $2 \cdot 1$-fins, P_{MR} and P_{LM}, contiguous to the trunk regions P_{RL}. As we mentioned above, the $2 \cdot 1$-fins are exceptional being confined by three boundaries instead of four. In particular, the fin P_{MR} is confined by the BCB and DFB boundaries

$$BC_{LR} = \left\{ p \in P : d_R = 1 - \frac{d_L}{a_R} \right\}, \tag{16}$$

$$DF_{MR} = \{ p \in P : d_R = d_L + a_R \}, \tag{17}$$

respectively, and the boundary defined by $d_L = 0$. The fin P_{LM} is confined by the BCB and DFB boundaries

$$BC_{RL} = \{p \in P : d_R = 1 - a_L d_L\} \tag{18}$$

$$DF_{LM} = \{p \in P : d_R = d_L + a_L\}, \tag{19}$$

respectively, and the boundary $d_R = 1$.

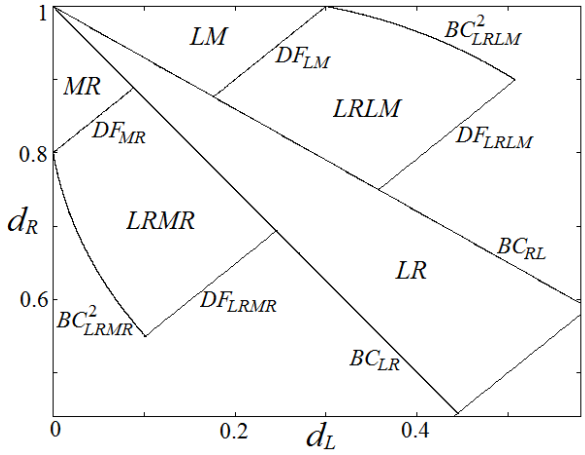

Figure 9: The $2 \cdot 1$-fins P_{MR} and P_{LM}, and $2 \cdot 2$-fins P_{LRMR} and P_{LRLM}, contiguous to the trunk regions P_{LR}. Here $a_L = 0.7$, $a_R = 0.8$ as in Fig.5.

Next, let us consider the $2 \cdot 2$-fins, P_{LRMR} and P_{LRLM}, which are also contiguous to the trunk regions P_{RL}. Applying the formulas given in Appendix B we get that the boundaries of the fin P_{LRMR} are given by the BCB curves satisfying the equations given below:

$$BC_{LR} = \left\{p \in P : d_R = 1 - \frac{d_L}{a_R}\right\}, \tag{20}$$

$$DF_{LRMR} = \left\{p \in P : d_R = d_L + a_R^2 a_L\right\}, \tag{21}$$

$$BC^1_{LRMR} = \{p \in P : d_R = d_L + a_R\}, \tag{22}$$

$$BC^2_{LRMR} = \left\{p \in P : d_L = \frac{d_R^2 - (a_R + 1)d_R + a_R}{a_R a_L + d_R}\right\}. \tag{23}$$

Note that $BC^1_{LRMR} = DF_{MR}$, that is, the DFB of the cycle LM occurs simultaneously with the BCB of the cycle $LRMR$ (see Fig.9). The fin P_{LRLM} is confined by the following boundaries:

$$BC_{RL} = \{p \in P : d_R = 1 - a_L d_L\}, \tag{24}$$

$$DF_{LRLM} = \{p \in P : d_R = d_L + a_R a_L^2\}, \tag{25}$$

$$BC^1_{LRLM} = \{p \in P : d_R = d_L + a_L\}, \tag{26}$$

$$BC^2_{LRLM} = \left\{p \in P : d_R = \frac{d_L^2 + a_L(d_L - a_R) - 1}{d_L - 1 - a_L a_R}\right\}, \tag{27}$$

and, as already remarked in the previous case, here also we have $BC^1_{LRLM} = DF_{LM}$ (see Fig.9).

4 Conclusions

In this work we have considered a pioneering model by Day and Shafer [9] which describes a business cycle by using a bimodal piecewise linear map. Our investigation shows how rich is the dynamic behaviors of the system, going from attracting cycles of any period, to robust chaotic intervals, depending on the parameters values. By using recently developed techniques, we have studied a typical bifurcation diagram and obtained analytically the border collision bifurcation curves that separate different periodicity regions, and degenerate flip bifurcation curves. The transition to chaos was also studied.

Complex dynamics are usually the consequence of the introduction of some nonlinearity in a system. Moreover, specially in economics, it is quite natural to have a nonlinearity coming simply by some constraint. That is, an economic model is often characterized by different functional definitions depending of some threshold reached by the dynamic variables (income, prices, etc.). In this way, the models are described by piecewise smooth systems (in place of smooth ones), whose theoretical results are still under study among scholars in Dynamical Systems. Thus, results similar to those of our model can be obtained in the study of other continuous piecewise linear systems.

Acknowledgments

The work of V. Avrutin was supported by the Marie Curie International Fellowship within the 7th European Community Framework Programme, project "Multiple-discontinuity induced bifurcations in theory and applications". The work of I. Sushko has been performed under the auspices of COST Action IS1104 "The EU in the new complex geography of economic systems: models, tools and policy evaluation".

References

[1] Avrutin, V., Schanz, M. & Gardini, L. [2010] "Calculation of bifurcation curves by map replacement," *Int. J. Bif. Chaos* **20**, 3105-3135.

[2] Banerjee, S., Karthik, M. S., Yuan, G. & Yorke, J. A. [2000], Bifurcations in one-dimensional piecewise smooth maps: theory and applications in switching circuits, IEEE Trans. Circ. Syst. I 47, 389-394.

[3] S. Banerjee, J.A. Yorke, C. Grebogi, Robust chaos, Physical Review Letters 80 (1998) 3049–3052.

[4] di Bernardo M, Budd CJ, Champneys AR, Kowalczyk P. Piecewisesmooth dynamical systems: theory and applications, applied mathematical sciences, vol. 163. London: Springer-Verlag; 2007.

[5] P. L. Boyland. Bifurcations of circle maps: Arnold tongues, bistability and rotation intervals. Comm. Math. Phys., 106(3):353-381, 1986.

[6] Day, R.H., 1982. Irregular growth cycles. American Economic Review 72, 406-414.

[7] Day, R.H., Complex Economic Dynamics, Volume I: An Introduction to Dynamical Systems and Market Mechanisms. Cambridge, MA: MIT Press, 1994.

[8] Day, R.H., Huang, W., 1990. Bull, bears and market sheep, Journal of Economic Behavior and Organization 14, 299-329.

[9] Day, R.H., Shafer, W., 1987. Ergodic fluctuations in deterministic economic models. Journal of Economic Behavior and Organization 8, 339-361.

[10] L. Gardini, F. Tramontana, V. Avrutin, M. Schanz "Border Collision Bifurcations in 1D PWL map and Leonov's approach." Int. J. Bifurcation and Chaos, 20(10) 3085-3104, 2010.

[11] L. Gardini, V. Avrutin, I. Sushko. Codimension-2 border collision bifurcations in one-dimensional discontinuous piecewise smooth maps. Int. J. Bifurcation and Chaos, 2014 (to appear).

[12] Gardini, L., Sushko, I. & Naimzada, A. [2008] "Growing through chaotic intervals," J. Econ. Th. 143, 541–557.

[13] Homburg, A. J. [1996] *Global aspects of homoclinic bifurcations of vector fields*, Memories of the American Math. Soc., Vol. 578 (Heidelberg: Springer).

[14] Huang W., Day, R.H., 1993. Chaotically switching bear and bull markets: the derivation of stock price distributions from behavioral rules. In: Day, R. and Chen, P. (eds): Nonlinear dynamics and evolutionary economics, Oxford University Press, Oxford, 169-182.

[15] Ito, S., Tanaka, S. & Nakada, H. [1979] "On unimodal transformations and chaos II," *Tokyo J. Math.* **2**, 241–259.

[16] Keener, J. P. [1980] "Chaotic behavior in piecewise continuous difference equations," *Trans. Am. Math. Soc.* **261**, 589–604.

[17] Leonov, N. N. [1959] "Map of the line onto itself," *Radiofisika* **3**, 942–956.

[18] Mackay R. S., Tresser C., Some Flesh on the Skeleton: the Bifurcation Structure of bimodal maps, Physica 27D (1987), 412-422.

[19] Y.L. Maistrenko, V.L. Maistrenko, L.O. Chua, Cycles of chaotic intervals in a time-delayed Chua's circuit, *Int. J. Bif. Chaos,* Vol.3 (1993) 1557–1572.

[20] Y.L. Maistrenko, V.L. Maistrenko, S.I. Vikul, L.O. Chua, Bifurcations of attracting cycles from time-delayed Chua's circuit*, Int. J. Bif. Chaos,* Vol. 5 (1995) 653–671.

[21] Milnor J., Remarks on Iterated Cubic Maps. Experimental Mathematics, Vol. 1 (1992), No. 1, 5-24.

[22] H.E. Nusse, J.A. Yorke, Border-collision bifurcations for piecewise smooth one-dimensional maps, *Int. J. Bif. Chaos,* Vol. 5 (1995) 189–207.

[23] A. Panchuk, I. Sushko, B. Schenke, V. Avrutin. Bifurcation Structure in Bimodal Piecewise Linear Map. *Int. J. Bif. and Chaos,* Vol. 23, No. 12 (2013).

[24] Ringland J., Tresser C., A Genealogy for Finite Kneading Sequences of Bimodal Maps on the Interval, Transactions of the American Mathematical Society, Vol. 347, No. 12, 1995, 4599-4624.

[25] I. Sushko, L. Gardini, Degenerate bifurcations and border collisions in piecewise smooth 1D and 2D maps, *Int. J. Bif. Chaos,* Vol. 20 (2010) 2045–2070.

[26] Sushko, I., Agliari, A. & Gardini, L. [2006] "Bifurcation structure of parameter plane for a family of unimodal piecewise smooth maps: Border-collision bifurcation curves," Chaos Solit. and Fract. 29, 756–770.

[27] I. Sushko, L. Gardini, K. Matsuyama "Superstable credit cycles and U-sequence" Chaos Solitons & Fractals, 59 (2014) 13–27.

[28] Takens, F. [1987] "Transitions from periodic to strange attractors in constrained equations," *Dynamical Systems and Bifurcation Theory*, eds. Camacho, M. I., Pacifico, M. J. & Takens, F. (Longman Scientific and Techical), pp. 399–421.

[29] Zhusubaliyev ZT, Mosekilde E. Bifurcations and chaos in piecewisesmooth dynamical systems. Singapore: World Scientific; 2003.

Appendix A

Consider a generic family of 1D continuous piecewise linear bimodal maps $g : \mathbb{R} \to \mathbb{R}$ defined as

$$g : x \mapsto g(x) = \begin{cases} g_L(x) = a_L x + \mu_L & \text{if} \quad x < d_L, \\ g_M(x) = a_M x + \mu_M & \text{if} \quad d_L \le x \le d_R, \\ g_R(x) = a_R x + \mu_R & \text{if} \quad x > d_R, \end{cases} \tag{28}$$

where $a_L > 0$, $a_R > 0$, $a_M < 0$, $d_L < d_R$.

To describe the period adding structure observed in the parameter space of map g consider first the basic cycles LR^{n_1} and RL^{n_1} belonging to the families $\Sigma_{1,1}$ and $\Sigma_{2,1}$ of complexity level one defined in (9). As stated in [23], the periodicity regions $P_{LR^{n_1}}$ and $P_{RL^{n_1}}$ of map g are defined as

$$P_{LR^{n_1}} = \{p : \Psi_{1,1}(a_L, a_R, \mu_R, d_R, n_1) < \mu_L < \Phi_{1,1}(a_L, a_R, \mu_R, d_L, n_1)\}, \tag{29}$$

$$P_{RL^{n_1}} = \{p : \Psi_{1,1}(a_L, a_R, \mu_L, d_L, n_1) > \mu_R > \Phi_{1,1}(a_L, a_R, \mu_L, d_R, n_1)\}, \tag{30}$$

where

$$\begin{aligned} \Phi_{1,1}(a_L, a_R, \mu, d, n_1) &= -\psi(a_R, n_1)\mu + \varphi(a_R, a_L, n_1)d, \\ \Psi_{1,1}(a_L, a_R, \mu, d, n_1) &= -\left(a_L + \psi(a_R, n_1 - 1)\right)\mu + a_R\varphi(a_R, a_L, n_1)d, \end{aligned}$$

with

$$\varphi(a, b, n) = \frac{1 - a^n b}{a^n}, \quad \psi(a, n) = \frac{1 - a^n}{(1 - a)a^n}.$$

These formulas are valid for the map f given in (2) substituting

$$\mu_L = 1 - a_L d_L, \quad \mu_R = -a_R d_R.$$

The periodicity regions related to cycles belonging to the families $\Sigma_{1,2}$ and $\Sigma_{2,2}$ of complexity level two given in (11) have the form

$$P_{\kappa^L_{n_2}(LR^{n_1})} = \{p : \Psi_{1,2}(a_L, a_R, \mu_R, d_R, n_1, n_2) < \mu_L < \Phi_{1,2}(a_L, a_R, \mu_R, d_L, n_1, n_2)\}, \tag{31}$$

$$P_{\kappa^R_{n_2}(LR^{n_1})} = \{p : \Psi_{2,2}(a_L, a_R, \mu_R, d_R, n_1, n_2) < \mu_L < \Phi_{2,2}(a_L, a_R, \mu_R, d_L, n_1, n_2)\}, \tag{32}$$

respectively, where $\kappa^L_{n_2}$ and $\kappa^R_{n_2}$ are defined in (10), and $\Phi_{1,2}$, $\Psi_{1,2}$, $\Phi_{2,2}$ and $\Psi_{2,2}$ are defined as

$$\begin{aligned} \Phi_{1,2}(a_L, a_R, \mu, d, n_1, n_2) &= -\psi(a_R, n_2)\mu - \\ &\quad - \frac{a_L a_R^{n_2}\psi(a_L a_R^{n_2+1}, n_1)\mu - \varphi(a_L a_R^{n_2+1}, a_L a_R^{n_2}, n_1)d}{a_R^{n_2}(1 + \psi(a_L a_R^{n_2+1}, n_1))}, \end{aligned}$$

$$\Psi_{1,2}(a_L, a_R, \mu, d, n_1, n_2) = -\frac{a_L a_R^{n_2}\left(a_L a_R^{n_2} + \psi(a_L a_R^{n_2+1}, n_1 - 1)\right)\mu}{a_R^{n_2}(1 + a_L a_R^{n_2} + \psi(a_L a_R^{n_2+1}, n_1) - 1)} -$$

$$-\psi(a_R,n_2)\mu+\frac{a_L a_R^{n_2+1}\varphi(a_L a_R^{n_2+1},a_L a_R^{n_2},n_1)d}{a_R^{n_2}(1+a_L a_R^{n_2}+\psi(a_L a_R^{n_2+1},n_1)-1)},$$

$$\Phi_{2,2}(a_L,a_R,\mu,d,n_1,n_2)=\frac{\varphi(a_L^{n_2}a_R,a_L^{n_2+1}a_R,n_1)d-a_L^{n_2}\left(1+\psi(a_L^{n_2}a_R,n_1)\right)\mu}{a_L^{n_2}\left(a_R+\psi(a_L,n_2)(1+\psi(a_L^{n_2}a_R,n_1))\right)},$$

$$\Psi_{2,2}(a_L,a_R,\mu,d,n_1,n_2)=$$

$$=\frac{a_R\varphi(a_L^{n_2}a_R,a_L^{n_2+1}a_R,n_1)d-\left(1+a_L^{n_2+1}a_R+\psi(a_L^{n_2}a_R,n_1-1)\right)\mu}{a_R+\psi(a_L,n_2)(1+a_L^{n_2+1}a_R+\psi(a_L^{n_2}a_R,n_1-1))}.$$

To get the periodicity regions of the cycles belonging to the families $\Sigma_{3,2}$ and $\Sigma_{4,2}$ (12) one has to interchange the indices L and R, as well as to change the inequality signs to the opposite ones in (32) and (31), respectively.

The periodicity regions of a complexity level k are obtained from the periodicity regions of the level $k-1$ by a recursive algorithm described in detail in [23].

Appendix B

Let us recall the analytic representation of the boundaries of $n\cdot k$-fins of map g given in (28), which have the common boundary with the trunk region $P_{LR^{n-1}}$. Consider first the fins P_σ contiguous to $P_{LR^{n-1}}$, corresponding to the attracting cycles $\sigma=(LR^{n-1})^{k-1}MR^{n-1}$, $n\geq 2$, $k\geq 2$. It is proved in [23] that any fin P_σ, if it exists[3], is confined by the boundaries defined as follows:

$$BC_{LR^{n-1}}=\left\{p\in P:\mu_L=-\frac{1-a_R^{n-1}}{(1-a_R)a_R^{n-1}}\mu_R+\frac{1-a_R^{n-1}a_L}{a_R^{n-1}}d_L\right\},$$

$$DF_\sigma=\{p\in P:a_M a_R^{k(n-1)}a_L^{k-1}=-1\},$$

$$BC_\sigma^1=\left\{p\in P:a_M a_R^{n-1}=\frac{a_L a_R^{n-1}((a_L a_R^{n-1})^{-k+1}-1)}{a_L a_R^{n-1}-1}\right\}$$

$$\begin{aligned}BC_\sigma^2 \;=\; &\left\{p\in P:a_R^{n-1}a_M\frac{(a_R^{n-1}a_L)^{k-1}-1}{a_R^{n-1}a_L-1}\left(\left(a_R^{n-2}a_L+\frac{a_R^{n-2}-1}{a_R-1}\right)\mu_R+a_R^{n-2}\mu_L\right)+\right.\\ &\left.a_R^{(n-1)k}a_M a_L^{(k-1)}d_R+\left(a_R^{n-2}a_M+\frac{a_R^{n-2}-1}{a_R-1}\right)\mu_R+a_R^{n-2}\mu_M=d_R\right\},\end{aligned}$$

where the BCB boundary $BC_{LR^{n-1}}$ which corresponds to $\mu_L=\Phi_{1,1}(a_L,a_R,\mu_R,d_L,n-1)$ given in (29), is common with the trunk region $P_{LR^{n-1}}$. The boundary DF_σ corresponds to the degenerate flip bifurcation, and BC_σ^1 and BC_σ^2 are related to two more BCBs of σ.

The $n\cdot k$-fin P_ρ attached to the trunk region $P_{LR^{n-1}}$ on the other side and related to the cycle $\rho=(LR^{n-1})^{k-1}LR^{n-2}M$, $k\geq 2$, is confined by the boundaries defined as follows:

[3] As a fin region may be an empty set.

$$BC_{RLR^{n-2}} = \left\{ p \in P : \mu_L = -\left(a_L + \frac{1 - a_R^{n-2}}{(1-a_R)a_R^{n-2}} \right) \mu_R + a_R \frac{1 - a_R^{n-1} a_L}{a_R^{n-1}} d_R \right\}$$

$$DF_\rho = \{ p \in P : a_M a_R^{k(n-1)-1} a_L^k = -1 \},$$

$$BC_\rho^1 = \left\{ p \in P : a_L a_M a_R^{n-2} = \frac{a_L a_R^{n-1} ((a_L a_R^{n-1})^{-k+1} - 1)}{a_L a_R^{n-1} - 1} \right\}$$

$$\begin{aligned} BC_\rho^2 \quad = \quad & \left\{ p \in P : a_R^{n-2} a_M a_L \frac{(a_R^{n-1} a_L)^{k-1} - 1}{a_R^{n-1} a_L - 1} \left(\frac{a_R^{n-1} - 1}{a_R - 1} \mu_R + a_R^{n-1} \mu_L \right) + \right. \\ & \left. a_R^{(n-1)k-1} a_M a_L^k d_L + \frac{a_R^{n-2} - 1}{a_R - 1} \mu_R + a_M a_R^{n-2} \mu_L + \mu_M = d_L \right\}. \end{aligned}$$

Here the boundary $BC_{RLR^{n-2}}$ corresponds to $\mu_L = \Psi_{1,1}(a_L, a_R, \mu_R, d_R, n-1)$ given in (29).

The boundaries of the fins contiguous to the trunk regions $P_{RL^{n-1}}$ are obtained interchanging the indexes L and R in the above expressions. The fin regions of the higher complexity levels are obtained using the map replacement technique (see [23] for details).

Applying these results to map f given in (2), we get that the fin region P_σ, associated with the cycles $\sigma = (LR^{n-1})^{k-1} M R^{n-1}$, $n \geq 2$, $k > 1$, is confined by the following boundaries:

$$BC_{LR^{n-1}} = \left\{ p \in P : d_L = a_R^{n-1} - \frac{(1 - a_R^{n-1}) d_R a_R}{(1 - a_R)} \right\}$$

$$DF_\rho = \left\{ p \in P : d_L = d_R - a_R^{k(n-1)} a_L^{k-1} \right\},$$

$$BC_\sigma^1 = \left\{ p \in P : d_L = d_R + \frac{a_L a_R^{n-1} - 1}{a_L ((a_L a_R^{n-1})^{1-k} - 1)} \right\},$$

$$\begin{aligned} BC_\sigma^2 \quad = \quad & \left\{ p \in P : d_R = -a_R^{n-1} \frac{(a_R^{n-1} a_L)^{k-1} - 1}{(a_R^{n-1} a_L - 1)(d_R - d_L)} \times \right. \\ & \times \left(- \left(a_R^{n-2} a_L + \frac{a_R^{n-2} - 1}{a_R - 1} \right) a_R d_R + a_R^{n-2} (1 - a_L d_L) \right) - \\ & \left. - \frac{a_R^{(n-1)k} a_L^{(k-1)} d_R}{d_R - d_L} - \left(- \frac{a_R^{n-2}}{d_R - d_L} + \frac{a_R^{n-2} - 1}{a_R - 1} \right) a_R d_R + \frac{a_R^{n-2} d_R}{d_R - d_L} \right\}. \end{aligned}$$

Accordingly, the $n \cdot k$-fin P_ρ related to the cycle $\rho = (LR^{n-1})^{k-1} L R^{n-2} M$, $k \geq 2$, is confined by the boundaries defined as

$$BC_{RLR^{n-2}} = \left\{ p \in P : 1 - a_L d_L = \left(a_L + \frac{1 - a_R^{n-2}}{(1-a_R)a_R^{n-2}} \right) a_R d_R + \right.$$
$$\left. + a_R \frac{1 - a_R^{n-1} a_L}{a_R^{n-1}} d_R \right\},$$

$$DF_\rho = \{ p \in P : d_L = d_R - a_R^{k(n-1)-1} a_L^k \},$$
$$BC_\rho^1 = \left\{ p \in P : d_L = d_R + \frac{a_L a_R^{n-1} - 1}{a_R((a_L a_R^{n-1})^{-k+1} - 1)} \right\}$$

$$BC_\rho^2 = \left\{ p \in P : d_L = -a_R^{n-2} a_L \frac{(a_R^{n-1} a_L)^{k-1} - 1}{(a_R^{n-1} a_L - 1)(d_R - d_L)} \times \right.$$
$$\times \left(-\frac{a_R^{n-1} - 1}{a_R - 1} a_R d_R + a_R^{n-1}(1 - a_L d_L) \right) - \frac{a_R^{k(n-1)-1} a_L^k d_L}{d_R - d_L}$$
$$\left. - \frac{a_R^{n-2} - 1}{a_R - 1} a_R d_R - \frac{a_R^{n-2}(1 - a_L d_L)}{d_R - d_L} + \frac{d_R}{d_R - d_L} \right\}.$$